Spring 2021

An Investigation on the Effect of the Chain Length of Glutamic Acid Oligomers on the Nucleation, Precipitate Growth, and Phase Transformation of Amorphous Calcium Phosphate to Crystalline Hydroxyapatite

Emma Harmon
elh63@zips.uakron.edu

An Investigation on the Effect of the Chain Length of Glutamic Acid Oligomers on the Nucleation, Precipitate Growth, and Phase Transformation of Amorphous Calcium Phosphate to Crystalline Hydroxyapatite

Emma Harmon, Putu Ustriyana[*]*, and Nita Sahai*[*]

Department of Chemistry, The University of Akron, Akron, Ohio 44325, United States

[*]School of Polymer Science and Polymer Engineering, The University of Akron, Akron, Ohio 44325, United States

Honors Project in Chemistry 3150:497

Abstract

Biomineralization is an important field of study focusing on mineralization by organisms from bacteria to vertebrates including processes, such as the formation of bone, cartilage, and dentin. This study investigated the effect that repeating units of the negatively charged amino acid, glutamic acid, in oligoglutamic acids of various lengths had on the mineralization behavior of hydroxyapatite. Hydroxyapatite (HA) is the key mineral in bone and dentin, which gives these materials their strength and stiffness. The degree of mineralization plays a key role in the strength and utility of biological tissues and is specific to the location and intended function of particular tissues. Located in the general regions of these tissues are proteins that help to regulate mineralization and direct tissue development. In this study, varying chain lengths of oligo-glutamic acid sequences were added to the reaction vessel of calcium and phosphate solutions to form amorphous calcium phosphate (ACP), a product which later phase-transforms to crystalline HA. Oligo(L-glutamic acid)$_n$ (n = 3, 7, 8,10) were tested using instantaneous addition of the phosphate stock solution into the calcium stock solution. The glutamic acid was found to delay the phase transformation of the ACP to crystalline HA and this effect increased as the chain length of the peptide increased. This is hypothesized to be due to the interaction of the negatively carboxylic acid groups on the glutamic acid oligomers with the positively charged calcium molecules before the addition of the phosphate, which eventually delayed the phase transformation of ACP to HA. The interaction of the peptide with the calcium atoms was thought to be stronger as chain length increased, given that there were more carboxylic acid units to interact with, causing the increased delay in phase transformation. This study worked as an extension to previous work conducted by Dr. Putu Ustriyana in which the same question was investigated, but the phosphate reagent was added in a slow, drop-wise fashion in that study

compared to instantaneous addition in the present work. Similar results in the delay of phase transformation were observed. Dr. Ustriyana's work showed the same trend observed in this study with the effect of the retardation of precipitation and phase transformation of ACP to HA increasing as chain length increased following the trend $Glu_3 < Glu_7 < Glu_8 < Glu_{10}$.[13] Dr. Ustriyana's work did show somewhat different results in the time point of phase transformation of ACP to HA for the control, Glu_3, and Glu_{10}, however due to a lack of comparable results, a firm conclusion on whether or not a true effect on the phase transformation delay due to the rate of phosphate addition did occur could not be drawn.

Background

Biomineralization is the process by which living organisms organize minerals in close association with bioorganic molecules for functional purposes within their bodies.[10] These biocomposite materials have properties superior to those of either bioorganic or inorganic phase alone. In this study, calcium phosphate minerals are of key interest. Calcium phosphate minerals play a large role within the human body, providing structure, protection, and storage to the body in the form of bones and teeth, for example. Bone and dentin are composites of HA in and around a scaffolding of collagen protein and associated with several non-collagenous proteins (NCPs). Understanding the pathways of calcium phosphate mineralization has been of great interest to the scientific and medical community, because understanding its mineralization habits can shed light on the mechanism behind pathologies such as osteoporosis.[1,13] Tissue engineering methods and devices also rely heavily on a deep understanding of how this process takes place.[1,13] For instance, scaffold devices and other drug delivery systems are being developed for

orthopedic application in the delivery of biologically activated calcium phosphate minerals to inspire healing and proper bone composition.[1]

Several factors play into the control of bone and dentin biomineralization within the environment of a vertebrate organism, one of which is the presence of NCPs.[10,13] The process of amorphous calcium phosphate (ACP) formation occurs within type I collagen organic matrices, which provide the 3-D environment for directing mineral formation while NCPs are control nucleation of an initial amorphous calcium phosphate phase, phase transformation to crystalline hydroxyapatite and crystal growth .[3,13] It has been noted that the concentration of mineral ions in the extracellular fluid of most vertebrates is great enough that HA, the most thermodynamically stable and crystalline form of calcium phosphate in the body, should form spontaneously.[3] This is not observed because of the presence of mineralization inhibitors in body fluids.[3,7,13] For instance, osteopontin is an NCP found in the matrix of bone that inhibits crystal formation of HA.[7,13] The significance of this particular protein is that is contains repeating units of a negatively charged nucleic acid under biological conditions.[7,13] This is the property that inhibits the phase transformation of ACP to HA. Other NCPs such as bone sialoprotein contain repeating units of other nucleic acids such as glutamic acid.[7,13] It is known and fairly widely documented that the presence of negatively charged nucleic acid sequences in NCPs inhibit crystal formation of ACP to HA, but the critical chain length effect is far less understood. The main goal of this study is to determine the effect that the chain length of glutamic acid oligomers has on the nucleation, growth, and phase transformation of ACP to HA, using various methods of analysis. Furthermore, it is known that the rate of mixing of reactants in a mineralizing solution influences the pathway of mineralization. Hence, a second goal of the present study is to compare the

effects of the rate of phosphate addition to a mineralizing system on the mineralization pathway. Here, I used an instantaneous addition of phosphate to the calcium solution compared to a parallel study in the Sahai laboratory, in which phosphate was added slowly, in a drop-wise manner.[13]

Transmission electron microscopy, TEM, was one of the techniques used to determine the time-point of phase transformation of the ACP to HA. TEM is an incredibly powerful type of microscopy that was first used in 1940 and has been vital in cellular and biological research ever since.[15] It can produce images with incredible magnification, clearly depicting nanoparticles less than 20nm in size.[4] TEM is made up of a few key components, an electron gun, a phosphor screen, and a camera.[6] These components are located within a vacuum sealed column and a compute with software is used to control the camera, electron beam, and image processing.[6] The sample to be analyzed is often either chemically fixed to sample disks, fixed in plastic sheets, cryo fixed, and more.[6] In this experiment, samples were fixed by drying liquid samples on copper mesh grids. TEM works by sending a concentrated beam of electrons from the electron gun and through a sample in a vacuum sealed column.[6] The electrons that pass through the sample are scattered and diffracted based on the structure of the sample particle and a resultant image is produced on the phosphor screen.[6] The camera captures the image and the computer software processes and displays it.[6] TEM was particularly useful for this study, because it allowed for detection of change on a very precise scale, so even slight changes in phase were detected. It is so strong, that is have been used to image specific organelles within cells many times.[4,15]

Dynamic light scattering, DLS, was another method used to monitor the growth and nucleation of ACP during the early stages of the precipitation reactions. DLS is a particularly powerful tool when looking to analyze proteins, nucleic acids, and other macromolecules.[12] Light scattering techniques have been used and documented in experimentation as early as 1868 and before by John Tyndall.[12] Years later, Malvern Instruments was the first company to commercialize the technique and produce a DLS machine for use in laboratory in situ experiments.[12] DLS also goes by a few other common names such as photon correlation spectroscopy, PCS, and Quasi-Elastic Light Scattering, QELS.[5] DLS machinery works by sending a beam of light directly through a sample held in a cuvette.[2] The laser beam of light then passes through the sample and scatters based on the location of particles in solution.[2] The beam is then stopped by a panel in the back of the machine and the scattered light rays are picked up and processed by a detector, hardware correlation unit, and computer software.[2] This gives information about the location of particles and dispersion habits of particles during an experiment.[2] In this case, it was used to determine the size distribution of macromolecules in the first 30 minutes of the precipitation experiment to determine how Glu of various chain lengths affected the distribution coefficient, dispersion habits, and particle growth of the precipitate.[2] Particles move and scatter light differently based on their size in a manner that corresponds to the Brownian motion principle.[2] This is what is generally used in the data processing step along with other kinetic principles for calculation.[2]

ICP-OES stands for inductively coupled plasma optical emission spectroscopy and it is a powerful analytical tool used to determination of the presence and concentrations of individual elements in a sample.[11] This technique was first developed for use in 1964 and worked off of previous qualitative analytical techniques that determined the presence of elements from flame

colors.[11] Plasma is an "ionized and luminous gas", often referred to as the fourth phase of matter, used in ICP-OES to interact with the ions in the sample with the free electrons and ions that it contains.[9] The plasma in this case is ionized argon gas and this ionization is accomplished through the use of an induction coil to heat the gas.[11] This is why it is referred to as inductively coupled plasma. When a sample comes in contact with this plasma, the elements in the sample interact with the ions and electrons to excite an outer valence shell electrons into an excited state.[11] When these electrons fall back down to a ground state the emit a wavelength of light that corresponds to the energy emission, the intensity of which is measured by a specific detector.[11] This is then correlated to a concentration, using calibration curves.[11] Another name for ICP-OES is inductively coupled plasma atomic emission spectroscopy.[8,9,11] One downfall of ICP-OES machinery is that it can be prime for errors caused by things like sample contamination for example.[14] It is important to understand these possible errors when relying on this technique for very accurate results.[8]

Materials and Methods

All chemical reagents used in this experiment were obtained from Sigma Aldrich (St. Louis, MO) unless otherwise noted. The peptide reagents, L-$(oligo)_n$-glutamic acid (n = 3, 7, 8, 10), were obtained from GenScript (Piscataway, NJ) and the purity was reported to be >95%. Solutions and stocks were made using nano-purified DI water with a resistivity of 18.2 MΩ⊕cm (Barnstead™ GenPure™ xCAD Plus, Thermo Scientific, Rockford, IL). All solutions were additionally filtered through a 0.1 μm filter before using as a reagent.

Stock Solution Preparation

Calcium stock solutions were prepared by dissolving calcium chloride ($CaCl_2$) salt in enough 10mM HEPES buffer (pH 7.4) to achieve a concentration of 50mM. Phosphate stock solutions were similarly made by dissolving ammonium phosphate ($(NH_4)_2HPO_4$) salt in enough 10mM HEPES buffer (pH 7.4) to achieve a concentration of 50mM. The calcium and phosphate stocks were made in volumes of 1L at a time using 1L volumetric flasks for volume measurement. Peptide stock solutions were made in concentrations of 0.1mM and 0.5mM. An additional peptide stock for Glu_7, Glu_8, and Glu_{10} was made with enough peptide to achieve a total carboxylic acid concentration in solution of 2mM. Some of the experiments were conducted using this fixed carboxylic acid concentration of peptide stock to help determine if the carboxylic acid unit was what was functional in retarding the mineral growth and phase transformation.

Precipitate Preparations

Precipitates for precipitation and crystallization analysis were made by adding HEPES buffer (pH 7.4), 50mM calcium stock, peptide stock, and 50mM phosphate stock to achieve a concentration ratio of calcium to phosphate of 4mM to 2.4mM respectively. For DLS experiments, the precipitate reactions were initially mixed using 2mL plastic centrifuge tubes as the reaction vessel and the solution was carefully transferred to a cuvette for analysis in the machine. For TEM and ICP-OES analysis, precipitates were made in plastic 1.5mL microcuvette tubes. The control group samples were made in the same manner, excluding the peptide addition step. For all samples, the calcium aliquot was added to the HEPES sample, with mixing using the pipette. The peptide was also added with gentle mixing and the phosphate aliquot was added in a single dose manner. The reaction vessel was then capped and quickly vortexed for ~2s. Depending on the analysis being performed, these resulting reaction solutions were either left to

age or used immediately for various analyses. All experiments were conducted at room temperature (~25℃).

Dynamic Light Scattering (DLS)

DLS analysis was conducted to determine particle size of the calcium phosphate precipitates using a Malvern Nano ZS Series (Malvern Panalytical, Westborough, MA) equipped with a 633 nm. A 4 mW HeNe laser was used for the measurement at 173° backscatter angle at 25 °C with 11 runs of 10 sec. There was a 5 s equilibration programmed for each measurement and the refractive indices of apatite and HEPES buffer used for data calculations were 1.630 and 1.332, respectively. The viscosity of the HEPES buffer was set to be 0.8910 cP. DLS was conducted on samples during the first 30 minutes of the precipitation process for the control group, all Glu chain lengths at 0.1mM, all Glu chain lengths at 0.5mM and the fixed carboxylic acid concentration 2mM for Glu_7, Glu_8, and Glu_{10}.

Transmission Electron Microscopy (TEM)

TEM was performed to characterize the size and morphology of the precipitates on a JEOL JSM-1230 (120 kV, Peabody, MA). TEM samples were made by producing precipitate samples of 500μL total volume as described before for Glu_3, Glu_7, Glu_8, and Glu_{10} for a peptide concentration of 0.5mM. The samples were left to react and analyzed at several time points (2min, 10min, 30min, 1hr, 3hr, 5hr, 8hr, 1 day). Once the aging process was complete, the reaction vessel was quickly vortexed and a 7μL aliquot was extracted and pipetted onto a formvar/carbon film-supported copper grid (300 mesh, Ted Pella, Inc., Redding, CA). The liquid

was allowed to sit on the mesh for 3 minutes and then the excess was gently blotted with a KIM wipe. The disc was allowed to fully air dry before TEM analysis.

Inductively Coupled Plasma - Optical Emission Spectroscopy (ICP-OES)

ICP-OES was conducted to determine calcium and phosphorus concentrations in solution at various time points using an ICP-OES (ICP-OES 720, Agilent, Santa Clara, CA). The concentration of Ca and P were measured at their respective wavelengths, 396.847 and 213.618 nm. Three measurements were taken and the average was reported. Samples for ICP-OES were prepared by first making precipitate samples for various time points (2min, 10min, 30min, 1h, 3h, 5h, 8h, 1d) using the precipitate preparation protocol described above. Samples were prepared for Glu_3, Glu_7, Glu_8, and Glu_{10} at concentrations of 0.1 mM total, 0.5mM total and also for 2mM total carboxylic acid. The precipitate samples were made in total volumes of 280µL and then centrifuged at 15,000 rpm for 5 min after the designated time point was reached. 190µL of the resulting supernatant was extracted and added to enough 5% (v/v) nitric acid solution to make a sample of 4mL total volume. The remaining supernatant was extracted from the resulting precipitate, and was then dissolved in 190µL of 5% nitric acid. This 190µL sample was then added to enough 5% nitric acid to reach 4mL total volume. These calcium phosphate solutions were then subjected to ICP-OES analysis to determine the rate of uptake of Ca and P as to confirm the formation of HA.

Results and Discussion

DLS analysis was used to determine the size distribution and growth of precipitated particles over the first 30 minutes of reaction. This was run for control samples and samples with Glu_3,

Glu_7, Glu_8, and Glu_{10}, The Glu_n concentrations tested included 0.1mM, 0.5mM, and 2mM total carboxylic acid. (**Figure 1)** below shows the patterns of particle growth over the course of the early stage of the reaction in the absence and presence of Glu_3, Glu_7, Glu_8, and Glu_{10}.

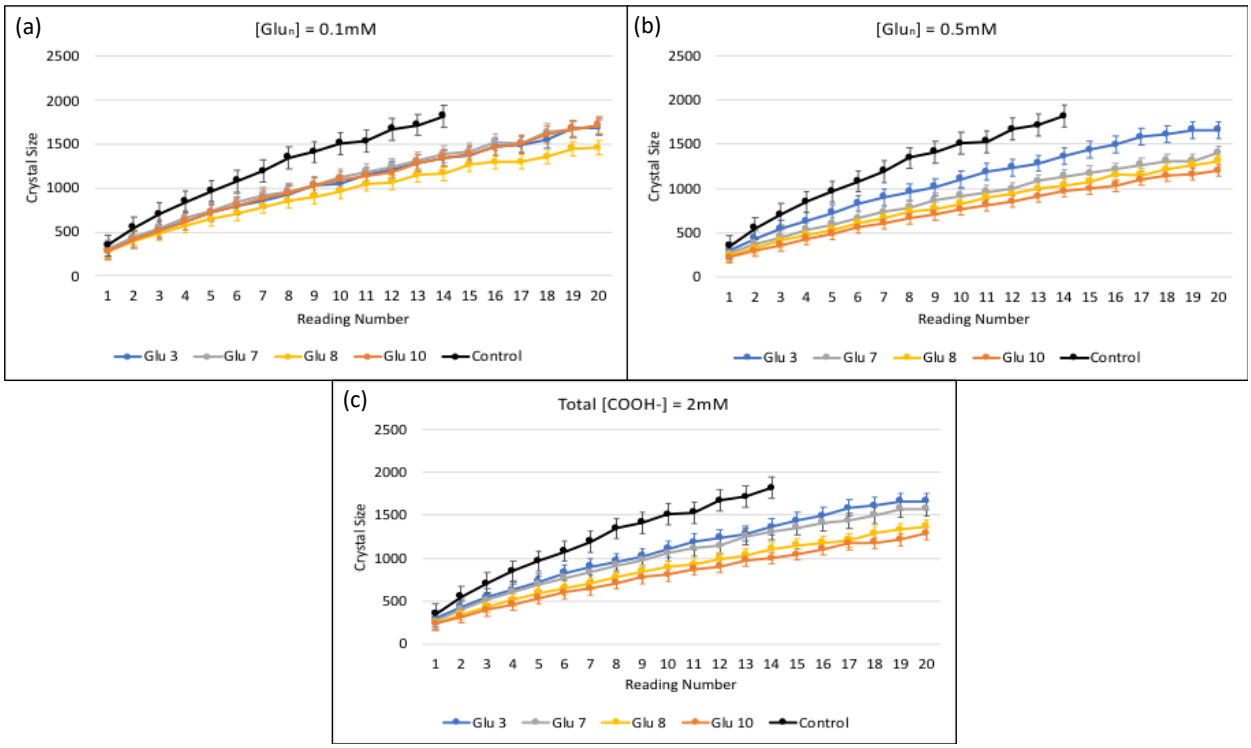

Figure 1. DLS particle size data recorded for the first 30 minutes of the reaction in the absence and presence of Glu_3, Glu_7, Glu_8, and Glu_{10} at concentrations of 0.1mM Glu_n (a) and 0.5mM Glu_n (b) and for 2mM total carboxylic acid (c).

Analysis of the results showed that the particles in the control group grew much more quickly than in the groups treated with peptide. This was consistent with the known retardation effect of negatively charged amino acids, like glutamic acid, on the nucleation and growth of ACP, which later went on to form HA. The 0.5mM concentration demonstrated that the longer the peptide chain, the stronger the retardation effect. The control group showed the most consistent size increase, followed by Glu_3 which is significantly slower. Compared to the control there was an average size decrease over time of 24.26% ±0.92% for Glu_3 treated samples at 0.5mM. This was

the smallest retardation effect of the Glu_n samples tested. Glu_7 followed with the next greater retardation effect, followed by Glu_8, and finally Glu_{10} with the greatest effect. Over the course of the experiment, the retardation effect for Glu_7, Glu_8 and Glu_{10} were 37.01% ±1.14%, 42.61% ±1.01%, and 47.75% ±0.94% on average compared to the control. These values, along with the standard deviation can be found below in (**Table 1)**.

Table 1. Percent retardation in calcium phosphate particle size increase over time for each Glu_n oligomer at 0.1mM concentration compared to the control sample without any oligoglutamic acid.

	Glu_3	Glu_7	Glu_8	Glu_{10}
Average	24.26%	37.01%	42.61%	47.75%
Standard Deviation	3.45%	4.26%	3.77%	3.53%
Standard Error	0.92%	1.14%	1.01%	0.94%

The 2mM total carboxylic acid concentration samples for $Glu_{7\text{-}10}$ also showed similar results. The shortest chain oligomer, Glu_7, had the smallest effect on the rate of crystal particle size increase compared to the control group. Glu_8 slowed the crystal growth slightly more and Glu_{10} slowed the crystal growth the most. This is the same pattern that was observed with the Glu_n= 0.5mM concentration systems. This result indicates that it is in fact the presence of contiguous carboxylic acids in the chain length and not the total number of carboxylic acid units present to interact with the calcium ions that are responsible for inhibiting the reaction with phosphate ions. If it were the number of carboxylic acid groups, then the retardation effect would be expected to be the same for Glu_3, Glu_7, Glu_8, and Glu_{10}, since the total number of acid groups was held constant in this trial.

The percentage retardation trends are reported below (**Table 2)**. Glu_7 slowed particle growth by an average of 28.62% ±0.6%, Glu_8 slowed growth by an average of 39.41% ±0.68% and Glu_{10}

slowed growth by 44.22% ±0.95% on average. Overall, it is clear that the retardation effect is weaker than in a [Glu_n] =0.5mM system. This result is ascribed to the fact that it is the peptide and corresponding chain length itself that retards the growth of the crystal, not the number of carboxylic acid groups.

Table 2. Percent retardation of the nucleation and crystal growth of the precipitate over time for each Glu chain sample compared to the control sample at 0.5mM concentration.

	Glu_3	Glu_7	Glu_8	Glu_{10}
Average	24.26%	28.62%	39.41%	44.11%
Standard Deviation	3.45%	2.23%	2.55%	3.54%
Standard Error	0.92%	0.60%	0.68%	0.95%

Finally, we also tested the effect of varying the concentration of $[Glu]_n$. At $[Glu]_n$ = 0.1mM for n = 3, 7, 8 and 10, the percentage of retardation was much smaller (Table 3) than at $[Glu]_n$ = 0.5mM (Table 1). This result suggests that a critical contraction exists for the retardation effect to be observed to a statistically significant magnitude.

Table 3. Percent retardation of the nucleation and crystal growth of the precipitate over time for each Glu chain sample compared to the control sample at 2mM total carboxylic acid concentration.

	Glu_3	Glu_7	Glu_8	Glu_{10}
Average	26.11%	23.36%	32.97%	26.21%
Standard Deviation	3.39%	3.74%	4.16%	2.39%
Standard Error	0.91%	1.00%	1.11%	0.64%

Furthermore, Glu_8 had the greatest effect on the retardation of the crystal growth, followed by Glu_{10}, then Glu_3, and finally Glu_7. The percentage by which growth was slowed by for Glu_3, Glu_7, Glu_8, and Glu_{10} were 26.11% ±0.91%, 23.36% ±1.00%, 32.97% ±1.11%, and 26.21% ±0.64% respectively. These results are inconsistent with the pattern observed for 0.5mM and 2mM total carboxylic acid, which suggests that either the concentration was too low for

observable effects to take place, or that the Glu chain length did not affect the initial stages of the reaction.

ICP-OES analysis was conducted for both the supernatant (**Figure 2, a, b**) as well as precipitates (**Figure 2c, d**) in the absence and presence of Glu_n at various concentrations (0.1mM, 0.5mM) and for total [COOH] = 2mM and sampled periodically up to 7 days. The results for the 0.1mM Glu_n systems are displayed below in (**Figure 2)**.

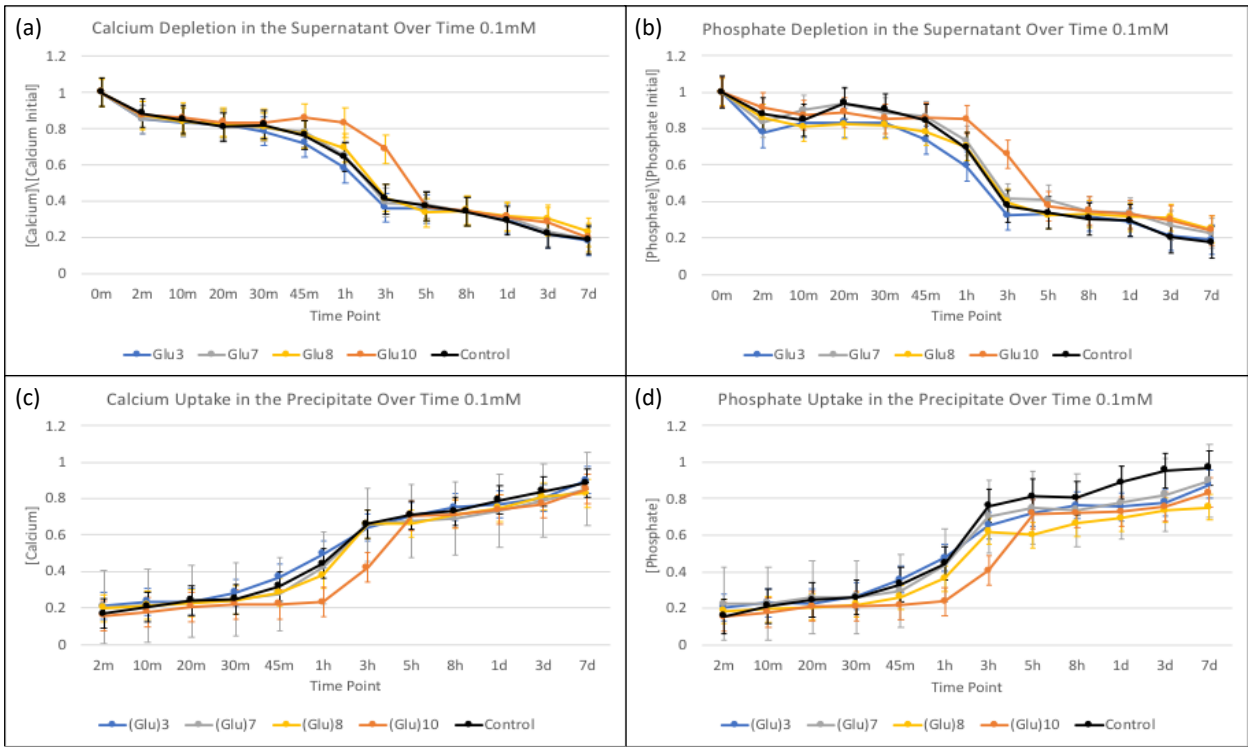

Figure 2. ICP-OES data of the calcium and phosphate concentrations in the supernatant (a, b) and precipitate (c, d) over time for the control system, Glu_3, and Glu_{10} and total [COOH] = 0.1mM for Glu_3, Glu_7, Glu_8, and Glu_{10}. Error bars represent the standard deviation of measurements on triplicate samples.

Both calcium and phosphate concentrations decrease in the supernatant solution over a 7-day period with two sharp drops. The first drop is interpreted to indicate the initial nucleation of ACP and the second likely corresponds to the phase transformation of ACP to HA. In **Figure 2** above, it is clear that samples in the presence of Glu_{10} experienced this phase transformation

much later than samples in the presence of the shorter oligoglutamic chains and the control. In detail, the second drop interpreted as the phase transformation for Glu_3 at 0.1mM and for the control was observed between 30 minutes and 3 hours. This is much sooner than that of Glu_{10}, which took place between 1 hour and 5 hours at 0.1mM concentration. Similar trends were observed the phosphate ion depletion and uptake of both ions by the precipitate as well.

The uptake of calcium and phosphate into the precipitates increased steadily over time with a sharp increase between 20 minutes and 3 h for the control and a delayed period of 1-5 h for Glu10. The shorter oligoglutamic acids show intermediate behavior. Thus, the inferred phase transformation is also delayed by the presence of oligoglutamic acid and is more effective as chain length increases.

Samples in the absence and presence of Glu_n at a total concentration of 0.5mM were also tested and similar trends to the 0.1mM trial were found, however the delay of the phase transformation was even greater. The results are displayed below in (**Figure 3)**.

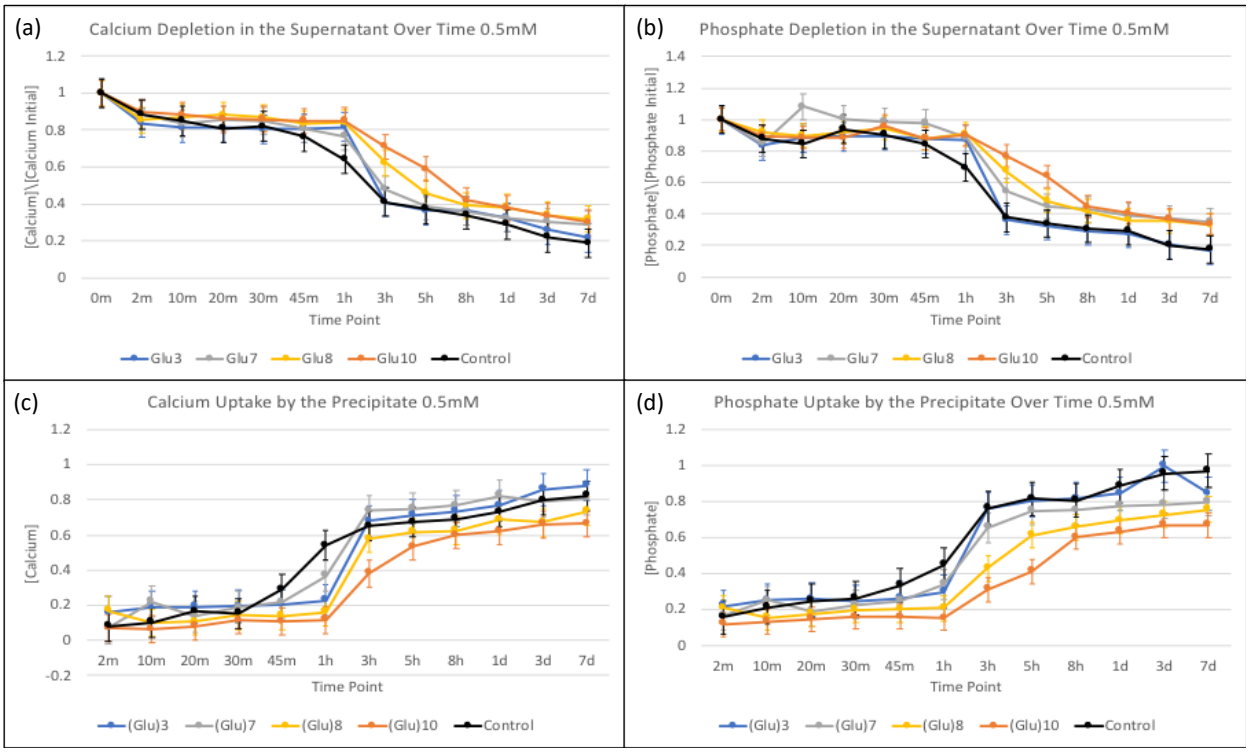

Figure 3. ICP-OES data of the calcium and phosphate concentrations in the supernatant (a,b) and precipitate (c,d) over time with error bars displayed for the control, Glu_3, and Glu_{10} in the presence and absence of 0.5mM Glu_3, Glu_7, Glu_8, and Glu_{10}.

Figure 3 shows the second drop in supernatant ion concentrations for Glu_3 and the control occurring between 30 minutes and 3 hours, however the second drop for Glu_{10} occurred between 1 hour and 8 hours. Not only did this second drop take place later, it lasted for longer, suggesting that the crystallization process occurred at a slower pace as well. This supports the effect shown in the DLS results that the retardation effect of ACP nucleation and phase transformation of ACP to HA increases as concentration of the oligoglutamic acid is increased from 0.1mM to 0.5mM.

The effect of various Glu_8 with a fixed carboxylic acid concentration of 2mM was also examined. Similar trends are seen as discussed above. The second drop in the ion concentration in the supernatant solution, inferred as ACP to HA phase transformation, appeared between 30 minutes and 3 hours for the control, but for Glu_3, the transformation appeared to occur between 1 hour and 3 hours, a shorter time window than previously observed (**Figure 4**). Glu_{10} showed this crystallization drop between 1 hour and 5 hours, which was more consistent with the results found in the 0.1mM trial. This is consistent with the total concentration of Glu_{10} and again gives rise to the concept that it is in fact the chain length (ie., presence of a contiguous series of carboxylate groups), and not the total number of carboxylic acid groups that contributes to the delay in crystal growth and mineralization of ACP to HA. If the concentration of carboxylic acid units were the reason for the retardation effect on the precipitation and phase transformation of ACP to HA, then **Figure 4** would have showed no difference in the rate of ion depletion/uptake for Glu_3, Glu_7, Glu_8, and Glu_{10}, because all of the samples contained the same concentration of COOH-. There would have been no difference in the displayed trend lines and the error bars would have showed no significant difference in the results for all Glu_n samples, given that the

COOH- concentration was held constant. Since this was not observed and the trends were shown to be significantly different, it is clear that the COOH- concentration is not what causes the retardation of effect of ACP growth and HA phase transformation.

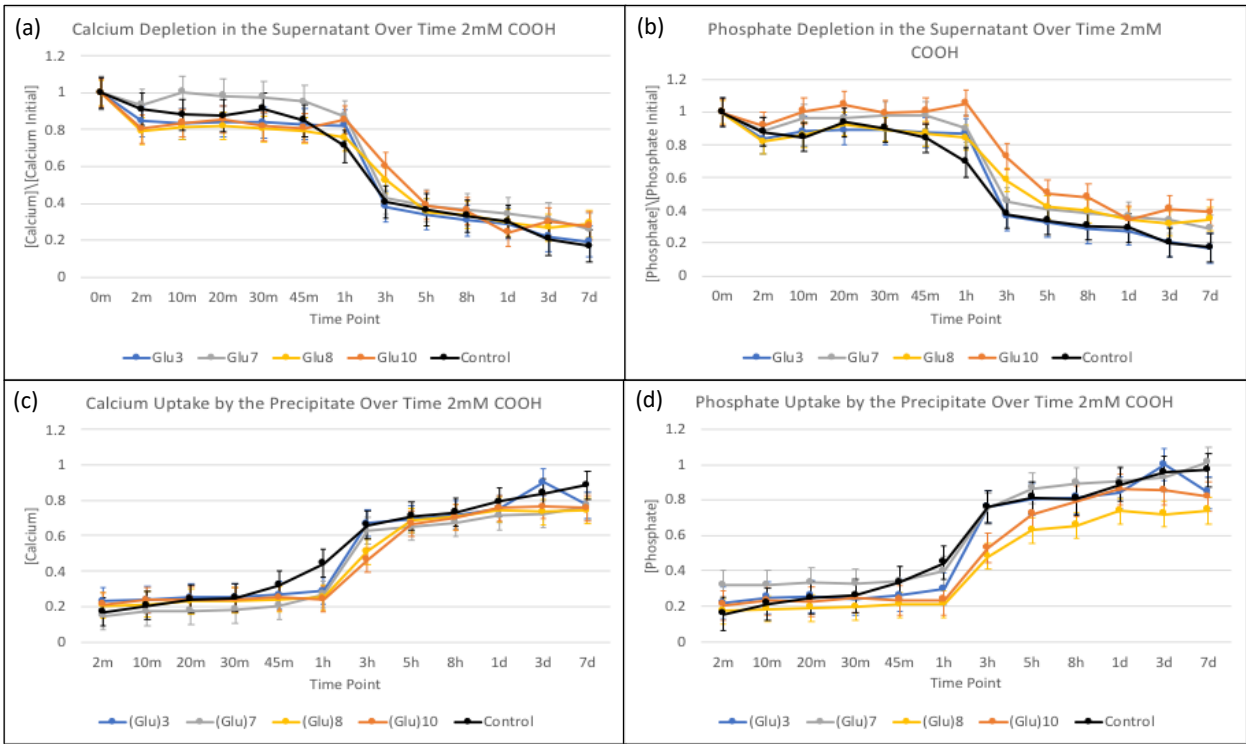

Figure 4. ICP-OES data of the calcium and phosphate concentrations in the supernatant (a,b) and precipitate (c,d) over time with error bars displayed for the control, Glu_3, and Glu_{10} in the presence and absence of 2mM total carboxylic acid concentration Glu_3, Glu_7, Glu_8, and Glu_{10}.

The important trend that ICP-OES shed light on in this experiment is the delay in phase transformation when in the presence of Glu oligomers of longer chains. Samples in the presence of Glu_7 and Glu_8 showed ICP-OES results that were consistent with what was observed in DLS. The retardation effect decreased in the sequence: $Glu_{10} > Glu_8 \sim Glu_7 > Glu_3$, where the difference between Glu_7 and Glu_8 was not statistically significant. This is why the comparison between the control, Glu_3 and Glu_{10} was the main focus of this section of the results. The following section on the TEM results also indicates more about the observed phase

transformation, and how it correlates with the observed second drop in ion concentration in the supernatant recorded via ICP-OES.

TEM was also used to track any changes in the morphology of the samples throughout the lifetime of the reaction for Glu_3 and Glu_{10} at 0.5mM concentration. TEM data was only collected for these two oligomers, because the maximum effect of chain length effect had been adequately established by the previous experiments. Brightfield TEM images of the control system are compared to those for 0.5mM Glu_3 and 0.5mM Glu_{10} systems (**Figure 5**).

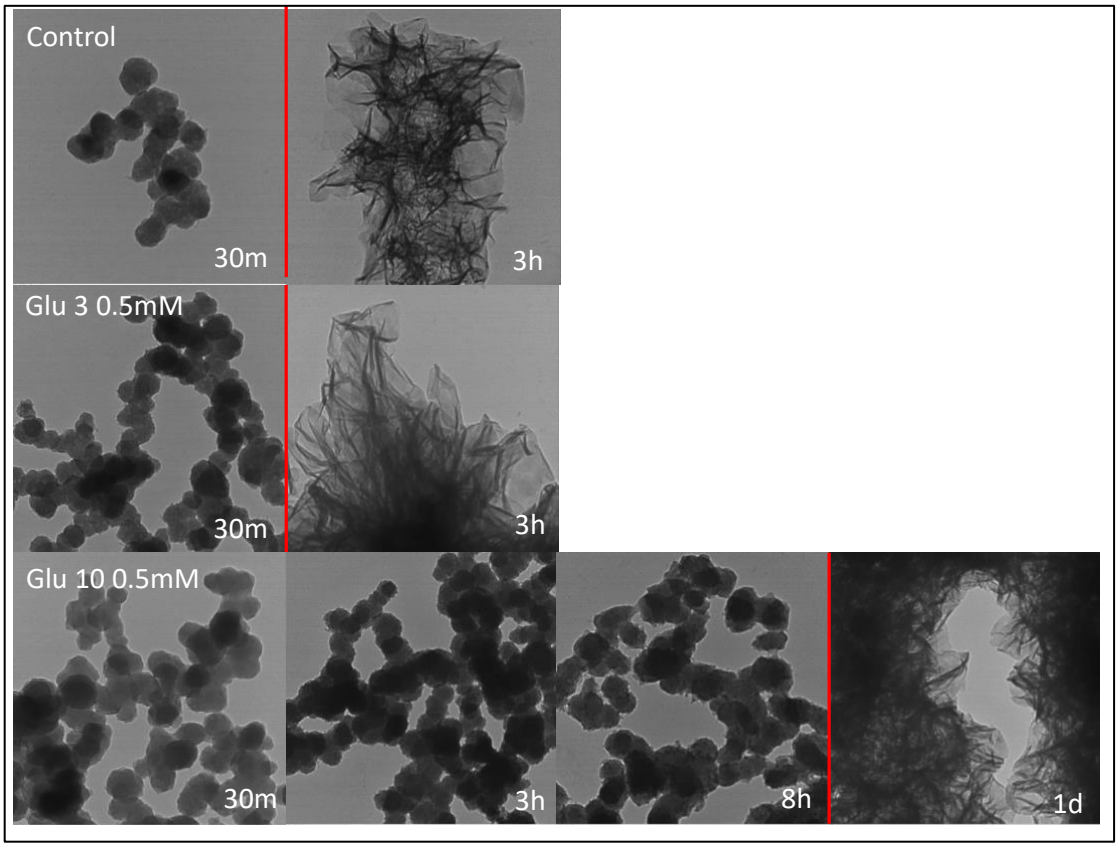

Figure 5. TEM images for samples in the presence and absence of Glu_3 and Glu_{10} at 0.5mM with the time point indicated and phase transformation indicated by the red line.

All three samples show spherical particles connected in chains at 30 minutes, consistent with nucleation and growth of ACP particles. By 3h, a wispy ribbon-like structure has appeared

for the control system sample. The change in morphology corresponds to a phase transformation to crystalline HA as determined by Selected Area Electron Diffraction (SAED) and synchrotron-based total X-Ray Scattering and Small Angle X-Ray Scattering on samples from very similar calcium phosphate precipitates in experiments where phosphate was added slowly in a drop-wise manner.[13] This is consistent with the trends demonstrated by the depletion of ions in the supernatant measured using ICP-OES, the second drop in supernatant ion concentration. This is what corresponded to the transformation of ACP to HA in this experiment. The Glu_3 sample showed the phase transformation at the same point as the control indicating little or no retardation effect. Glu_{10} samples showed small spike-like projections from the surface of the ACP particles at 8h which are interpreted as the beginning of crystallization with full phase transformation occurring by day 1. Thus, Glu_{10} retarded the ACP to HA phase transition compared to Glu_3 or the control, consistent with the ICP-OES data.

Dr. Ustriyana's work on this topic with the addition of phosphate being dropwise showed very similar results. The trend of the delay of phase transformation increasing with peptide chain length in the manner, $Glu_3 < Glu_7 < Glu_8 < Glu_{10}$, held true for her results.[13] Dr. Ustriyana's results did differ slightly from those found in this study in that the phase transformation time point for Glu_{10} was slightly less delayed. This study found it to occur in TEM results at the timepoints showed below in **Table 4**.

Table 4. Time point of observed phase transformation of ACP to HA for Dr. Ustriyana's results with [COOH] = 2mM and the results of this study with [Glu_n]= 0.5mM.

	Time Point HA Viewed	
Glu Sample	Ustriyana	Harmon
Control	3h	3h
Glu_3	3h	3h
Glu_{10}	8h	1d

It is not possible to perfectly compare the results, however, given that the concentration of Glu_n differed in both studies. This study focused on [Glu_n] = 0.5mM for TEM, while Dr. Ustriyana held [COOH] = 2mM for TEM comparison.[13] The general trend was still displayed.

ICP-OES results for [Glu_n] = 0.1mM were also compared for comparison of the phase transformation delay trends as well. The results are displayed below in **Table 5**.

Table 5. Time point of observed phase transformation as indicated by the end of sharp ion depletion from ICP-OES for Dr. Ustriyana's results and the results of this study with [Glu_n]= 0.1mM.

	Time Point End of Ion Depletion	
Glu Sample	Ustriyana	Harmon
Control	3h	3h
Glu_3	3h	3h
Glu_{10}	8h	5h

Results for ICP-OES again showed a very similar trend. Dr. Ustriyana's results differed in that the end of the second drop in ICP-OES indicating full phase transformation occurred slightly later than for the results of this study.[13] Ideally, TEM results with the same peptide concentration would be compared, but since those results were not obtained, ICP-OES results were used for comparison. The difference could be significant in that the mechanism for phase transformation delay could be slightly more effective when the phosphate reagent is added dropwise instead of instantaneously. To confirm whether a true difference in this time point is present between the two styles of reagent addition, further ICP-OES and TEM data would need to be gathered for comparison.

Conclusions

The purpose of this study was to better understand the effect that the chain length of glutamic acid-based oligomers had on the retardation of the nucleation, growth and phase transformation

of ACP to crystalline HA. Oligoglutamic acids did not affect the nucleation rate of ACP but retarded the growth of ACP particles up to at least 30 minutes as monitored by DLS and ICP-OES. The effect was enhanced at higher concentrations of the oligomers and longer chain lengths. The oligoglutamic acids also delayed the phase transition of ACP to crystalline HAP with longer oligomers having a greater effect. Interestingly, the effects on both ACP particle growth and phase transition were dependent on chain length (presence of contiguous carboxylic acids in the oligomer) rather than the total concentration of -COOH groups. This finding has implications for the mechanism of oligoglutamic acid-induced retardation of calcium phosphate mineralization mechanism and will be explored further in future studies by the Sahai group. Knowledge of how to properly control and target the mineralization of tissue can have great clinical applications. The present results can be used to further develop treatments for pathologies regarding bone mineralization.

Acknowledgements

I would like to thank Dr. Nita Sahai, the University of Akron, and the Department of Polymer Science for allowing me to conduct research in the lab and providing me with guidance and funding along the way. I would also like to especially thank Dr. Putu Ustriyana for generously sharing a part of her project, being a mentor to me over the course of my undergraduate degree and for inspiring me to love the process of learning through research. Thank you to Dr. Adam Smith and Dr. Sailaja Paruchuri for teaching me during my time at the university and for reading and advising me on this project. This project has been a knowledge filled journey and these special mentors have been a vital part of this work being produced. For that I am incredibly grateful to them.

References

(1) Eliaz, N.; Metoki, N. Calcium Phosphate Bioceramics: A Review of Their History, Structure, Properties, Coating Technologies and Biomedical Applications. *Materials (Basel).* **2017**, *10* (4). https://doi.org/10.3390/ma10040334.

(2) Falke, S.; Betzel, C. *Dynamic Light Scattering (DLS): Principles, Perspectives, Applications to Biological Samples*; Springer International Publishing, 2019; Vol. 8. https://doi.org/10.1007/978-3-030-28247-9.

(3) George, A.; Veis, A. Phosphorylated Proteins and Control over Apatite Nucleation, Crystal Growth, and Inhibition. *Chem. Rev.* **2008**, *108* (11), 4670–4693. https://doi.org/10.1021/cr0782729.

(4) Guzzinati, G.; Altantzis, T.; Batuk, M.; De Backer, A.; Lumbeeck, G.; Samaee, V.; Batuk, D.; Idrissi, H.; Hadermann, J.; Van Aert, S.; et al. Recent Advances in Transmission Electron Microscopy for Materials Science at the EMAT Lab of the University of Antwerp. *Materials (Basel).* **2018**, *11* (8). https://doi.org/10.3390/ma11081304.

(5) Malm, A. V.; Corbett, J. C. W. Improved Dynamic Light Scattering Using an Adaptive and Statistically Driven Time Resolved Treatment of Correlation Data. *Sci. Rep.* **2019**, *9* (1), 1–11. https://doi.org/10.1038/s41598-019-50077-4.

(6) Mariano, R. G.; Yau, A.; Mckeown, J. T.; Kumar, M.; Kanan, M. W. Comparing Scanning Electron Microscope and Transmission Electron Microscope Grain Mapping Techniques Applied to Well-Defined and Highly Irregular Nanoparticles. *ACS Omega* **2020**. https://doi.org/10.1021/acsomega.9b03505.

(7) Morgan, S.; Poundarik, A. A.; Vashishth, D. Do Non-Collagenous Proteins Affect Skeletal Mechanical Properties? *Calcif. Tissue Int.* **2015**, *97* (3), 281–291. https://doi.org/10.1007/s00223-015-0016-3.

(8) Nyika, J.; Onyari, E.; Dinka, M. O.; Mishra, S. B. A Comparison of Reproducibility of Inductively Coupled Spectrometric Techniques in Soil Metal Analyses. *Air, Soil Water Res.* **2019**, *12*. https://doi.org/10.1177/1178622119869002.

(9) Ohls, K.; Bogdain, B. History of Inductively Coupled Plasma Atomic Emission Spectral Analysis: From the Beginning up to Its Coupling with Mass Spectrometry. *J. Anal. At. Spectrom.* **2016**, *31* (1), 22–31. https://doi.org/10.1039/c5ja90043c.

(10) Shastri, V. P. Biomineralization: A Confluence of Materials Science, Biophysics, Proteomics, and Evolutionary Biology. *MRS Bull.* **2015**, *40* (6), 473–477. https://doi.org/10.1557/mrs.2015.118.

(11) Spectra, A. E. *10 . 7 : Atomic Emission Spectroscopy*; Harvey, D., Ed.; LibreTexts, 2020.

(12) Stetefeld, J.; McKenna, S. A.; Patel, T. R. Dynamic Light Scattering: A Practical Guide and Applications in Biomedical Sciences. *Biophys. Rev.* **2016**, *8* (4), 409–427. https://doi.org/10.1007/s12551-016-0218-6.

(13) Ustriyana, P.; Harmon, E.; Chen, K.; Michel, F. M.; Sahai, N. Oligo(l -Glutamic Acids) in Calcium Phosphate Precipitation: Chain Length Effect. *J. Phys. Chem. B* **2020**, *124* (29), 6278–6287. https://doi.org/10.1021/acs.jpcb.0c01689.

(14) Valavanidis, A. Dietary Supplements: Beneficial to Human Health or Just Peace of Mind? A Critical Review on the Issue of Benefit/Risk of Dietary Supplements. *Pharmakeftiki* **2016**, *28* (2), 60–83.

(15) Winey, M.; Meehl, J. B.; O'Toole, E. T.; Giddings, T. H. Conventional Transmission Electron Microscopy. *Mol. Biol. Cell* **2014**, *25* (3), 319–323. https://doi.org/10.1091/mbc.E12-12-0863.

Appendix 1

Safety considerations

Several safety measures were taken to protect the researcher in this project. This included wearing latex-free gloves, splash proof safety goggles, close-toed shoes, long pants, tied back hair, and lab coats during all experimental procedures. Acids and bases were stored in glass containers and used in specific hoods to minimize the likelihood of contamination. Nitric acid solutions were used in the hood to minimize the likelihood of lung damage from inhalation of mists or dust particles. There was also an emergency eyewash and shower station located nearby for emergency use in the case of an accidental spill. Samples were also neutralized thoroughly with a basic solution and disposed of in an acid biohazard container. Due to its nature as a fire accelerant, a fire blanket was also kept nearby when in use. Very similar measures were taken when KOH was being used. It was used in the preparation of the peptide stocks and the same general safety measures were necessary due to its caustic nature and negative impacts on the respiratory tract, eyes and skin when contact occurred. Again, similar precautions were taken when handling calcium chloride and ammonium phosphate, however ammonium phosphate was slightly less dangerous. TEM was deemed very safe for use and posed very little radiation exposer danger. No special sign postage or personnel monitoring was required. Gloves were worn, as they were recommended simply because chemical samples were being handled. The vacuum column was properly locked and unlocked to avoid any escape of radiation or damage to the machine. For ICP-OES use, the radiation potential was not of health concern according to the MSDS. The nitric acid was identified as a caustic material that was potentially dangerous to one's health when in contact with skin, eyes or respiratory tract. Precautions were followed as

described above to neutralize this danger. DLS showed no significant safety concerns. Proper PPE was worn due to chemicals being handled to set up initial reaction vessels.